J. Membrane Biol. 177, 231–242 (2000)
DOI: 10.1007/s002320010006

The Journal of
Membrane
Biology

Mechanism of Shrinkage Activation of Nonselective Cation Channels in M-1 Mouse Cortical Collecting Duct Cells

J.-P. Koch[1,2], C. Korbmacher[2]
[1]Zentrum der Physiologie, Johann Wolfgang Goethe-Universität, Theodor Stern-Kai 7, D-60590 Frankfurt am Main, Germany
[2]University Laboratory of Physiology, Parks Road, Oxford, OX1 3PT UK

Received: 3 May 2000/Revised: 6 July 2000

Abstract. It has previously been shown that osmotic cell shrinkage activates a nonselective cation (NSC) channel in M-1 mouse cortical collecting duct cells [54] and in a variety of other cell types [20]. In the present study we further characterized the shrinkage-activated NSC channel in M-1 cells and its mechanism of activation using whole-cell current recordings. Osmotic cell shrinkage induced by addition of 100 mM sucrose to the bath solution caused a 20-fold increase in whole-cell inward currents from −10.8 ± 1.5 pA to −211 ± 10.2 pA (n = 103). A similar response was observed when cell shrinkage was elicited using a hypo-osmotic pipette solution. This indicates that cell shrinkage and not extracellular osmolarity *per se* is the signal for current activation. Cation substitution experiments revealed that the activated channels discriminate poorly between monovalent cations with a selectivity sequence NH_4 (1.2) ≥ Na^+ (1) ≈ K^+ (0.9) ≈ Li^+ (0.9). In contrast there was no measurable permeability for Ca^{2+} or Ba^{2+} and the cation-to-anion permeability ratio was about 14. The DPC-derivatives flufenamic acid, 4-methyl-DPC and DCDPC were the most effective blockers followed by LOE 908, while amiloride and bumetanide were ineffective. The putative channel activator maitotoxin had no effect. Current activation was dependent upon the presence of intracellular ATP and Mg^{2+} and was inhibited by staurosporine (1 μM) and calphostin C (1 μM). Moreover, cytochalasin D (10 μM) and taxol (2 μM) reduced the current response to cell shrinkage. These findings suggest that the activation mechanism of the shrinkage-activated NSC channel involves protein kinase mediated phosphorylation steps and cytoskeletal elements.

Key words: Cell shrinkage — Volume regulation — Patch clamp — Nonselective cation channels — Cytoskeleton

Correspondence to: C. Korbmacher

Introduction

Calcium-activated NSC channels have been described in a large variety of cell types [45]. They are usually silent in cell-attached patches and in the whole-cell configuration, but can be activated in excised inside-out patches by calcium concentrations in the micro- to millimolar range at the cytosolic surface. Since the other characteristic feature of the NSC channels is their sensitivity to inhibition by millimolar concentrations of ATP in the cytosol, it has been questioned whether these channels can be activated in normal living cells which typically maintain high intracellular ATP levels and submicromolar intracellular calcium concentrations.

We could recently demonstrate that cell shrinkage is an alternative way to activate this channel. Indeed, exposure to extracellular hyperosmolarity activates NSC channels in various cell types [6, 20, 54]. We identified the single channel properties of the shrinkage-activated nonselective cation (NSC) channel in several epithelial and nonepithelial cell lines including the M-1 mouse renal cortical collecting duct (CCD) cell line [20, 54]. Its single-channel conductance, ion selectivity, and inhibition by flufenamic acid suggest that the shrinkage-activated NSC channel is identical to the NSC channel found in inside-out patches of M-1 cells [25]. This channel belongs to the emerging family of calcium-activated NSC channels [45] consistent with the expected ubiquitous nature of the shrinkage-activated NSC channel.

Indeed, the shrinkage-activated NSC channels may be as widely distributed as the ubiquitously expressed swelling-activated Cl^- channel [39, 49] and they may also play a role in cell volume regulation. Several mem-

brane transport processes including ion channels have been shown to be activated in response to osmotic cell swelling or cell shrinkage (*for review:* [28]). However, the mechanisms of their activation are not fully understood and are believed to involve a large number of signaling pathways [16, 40].

There have been numerous studies to investigate the activation mechanism of swelling-activated Cl^- channels and it has been suggested that ATP-dependent mechanisms, phosphorylation and dephosphorylation steps, additional regulatory proteins, and cytoskeletal elements may all be involved. However, it is probably fair to say that many questions regarding the molecular details of the activation mechanism of the swelling-activated Cl^- channel remain unknown and that the molecular identity of the underlying channels is still elusive [39, 48, 49]. Even less is known about the activation mechanism and molecular nature of the shrinkage-activated NSC channel [20].

The aim of the present study was to further characterize the shrinkage-activated NSC channel in M-1 mouse CCD cells and to investigate its mechanism of activation. In particular we wanted to investigate whether extracellular hyperosmolarity *per se* or cell shrinkage was the trigger of NSC channel activation. Moreover, we further investigated its ion selectivity, inhibitor sensitivity, and the role of intracellular calcium and intracellular ATP in its activation. Finally, we looked for the possible involvement of a phosphorylation step and the cytoskeleton in its activation by shrinkage.

Materials and Methods

Cell Culture

The M-1 mouse cortical collecting duct cell line (ATCC 2038-CRL, American Type Culture Collection, Rockville, MD) was originally obtained from Dr. Fejes-Tóth [47]. Cells were used from passage 10 to 36 and were handled as described previously [24, 29]. Cells were maintained in a 5% CO_2 atmosphere at 37°C in PC1 culture medium (BioWhittaker, Walkersville, MD) supplemented with 2 mM L-glutamine, 100 U/ml penicillin, and 100 μg/ml streptomycin. For patch-clamp experiments 5% fetal calf serum (FCS, Seromed/Biochrom KG, Berlin, Germany) was added to the medium in which cells were seeded onto small pieces of glass cover slips. Cells were used one day after seeding.

Patch-Clamp Technique

The ruptured-patch whole-cell configuration of the patch-clamp technique was used [13] and experimental procedures were essentially as described previously [29]. Experiments were performed at room temperature. An EPC-9 patch-clamp amplifier (HEKA Elektronik, Lambrecht, Germany) was used to measure whole-cell currents or membrane voltage (V_m). An ATARI computer system was used to operate the EPC-9 amplifier and for data acquisition and analysis. Cells were viewed through a 40× objective of a Nikon TMS inverted microscope (Nikon GmbH, Düsseldorf, Germany) equipped with Hoffman modulation optics (Modulation Optics, Greenvale, NY) and cell diameter was estimated using a micrometer grid. Patch pipettes were pulled from Clark glass capillaries (Clark Electromedical Instruments, Pangbourne, UK) and had a resistance of 3.57 ± 0.05 MΩ ($n = 404$) in NaCl/Ringer when filled with NaCl/EGTA pipette solution (*see below*). The reference electrode was an Ag/AgCl pellet bathed in the same solution as that used in the pipette, and connected to the bath via an agar/pipette-solution bridge in the outflow path of the chamber. Liquid junction potentials occurring at the bridge/bath junction were measured using a 3M KCl flowing boundary electrode and were 5, −3, 2, −4, 5, or 4 mV when bath Na^+ was replaced by NMDG, K^+, Li^+, NH_4^+, Ca^{2+}, or Ba^{2+}, respectively. For data analysis the measured V_m values were corrected accordingly and in the whole-cell current recordings the pipette holding potential was corrected for liquid junction potentials as appropriate. Upward (positive) current deflections correspond to cell membrane outward currents. The membrane capacitance (C_m) and series resistance (R_s) were estimated by nulling capacitive transients using the automated EPC-9 compensation circuit. C_m averaged 8.4 ± 0.2 pF ($n = 387$). The corresponding R_s values averaged 12.1 ± 0.5 MΩ ($n = 387$); R_s was not compensated. For data analysis the current data were filtered at 200 Hz and were read into the computer via the ITC-16 interface of the EPC-9 patch-clamp amplifier at a sample rate of 1 kHz. Single channel current amplitudes were estimated from amplitude histograms. Data were analyzed using the program 'Patch for Windows' written by Dr. Bernd Letz (HEKA Elektronik, Lambrecht/Pfalz, Germany). Data are given as mean values ± SEM, significances were evaluated by the appropriate version of Student's *t*-test.

Solutions and Chemicals

The standard bath solution was NaCl-solution (in mM): 140 NaCl, 5 KCl, 1 $CaCl_2$, 1 $MgCl_2$, and 10 Hepes (adjusted to pH 7.5 with NaOH; the osmolarity was *ca.* 300 mosmol/l). Extracellular hyperosmolarity (*ca.* 400 mosmol/l) was achieved by adding 100 mM sucrose to the bath solution without changing its ionic composition. When using hypo-osmolar pipette solutions (*see below*), NaCl in the bath solution was reduced to 90 mM (*ca.* 200 mosmol/l) and addition of 100 mM sucrose was used to achieve the same osmolarity as the standard bath solution (*ca.* 300 mosmol/l). For testing monovalent cation selectivity Na^+ was replaced by an equal amount of K^+, Li^+, NH_4^+ or NMDG (N-methyl-D-glucamine). For testing divalent cation selectivity NaCl was replaced by 75 mM $CaCl_2$ or $BaCl_2$ and the osmolarity was corrected by adding 75 mM D-mannitol. To all bath solutions 5 mM glucose was added before usage.

Pipettes were filled with NaCl/EGTA-solution (in mM: 145 NaCl, 1 EGTA, 1 $MgCl_2$, 10 Hepes adjusted to pH 7.5 with NaOH; the osmolarity was *ca.* 300 mosmol/l). Hypo-osmolar pipette solution (*ca.* 200 mosmol/l) contained 95 mM NaCl. Stronger calcium buffering was achieved by using pipette solutions containing 10 mM EGTA or 10 mM BAPTA. In these pipette solutions 2 mM $MgCl_2$ was added to prevent a critical fall of the free Mg^{2+} concentration and NaCl was reduced to 115 mM to adjust osmolarity and to account for the additional NaOH necessary for pH adjustment. The free Mg^{2+} concentration in the various pipette solutions was calculated using the program 'Chelator' (Theo J.M. Schoenmakers, Department of Animal Physiology, University of Nijmegen, Toernooiveld, NL-6525 ED Nijmegen, Netherlands) and was 0.94 mM with 1 mM EGTA, 0.60 mM with 10 mM EGTA, and 1.52 mM with 10 mM BAPTA. To obtain a Mg^{2+}-free pipette solution Mg^{2+} was omitted from the pipette solution and 10 mM EDTA were added. In one set of experiments, cells were ATP-depleted by a 62 ± 10 min preincubation in NaCl-bath solution containing 100 nM rotenone and 5 mM 2-deoxyglucose instead of glucose as previously de-

scribed [17, 34]. Alternatively, 2.5 μM of carbonyl-cyanide-p-(trifluoromethoxy)phenylhydrazone (FCCP) was used instead of rotenone to achieve ATP depletion. In these ATP-depletion experiments M-1 cells were kept in the continuous presence of rotenone (or FCCP) and 2-deoxyglucose in the bath and pipette solution.

All chemical agents were purchased from Sigma (Deisenhofen, Germany), except for Maitotoxin (Calbiochem, Bad Soden, Germany), and LOE908 (Boehringer Ingelheim, Germany). Water-insoluble substances were dissolved in DMSO (final concentration not exceeding 0.25%).

Results

Extracellular Hyperosmolarity and Intracellular Hypo-osmolarity Stimulate M-1 Whole-Cell Currents

As shown in Fig. 1*A* extracellular hyperosmolarity stimulated M-1 whole-cell currents consistent with our previous findings [54]. Under iso-osmolar control conditions at a holding potential of −40 mV inward currents were small (−10.8 ± 1.5 pA, $n = 103$), and replacement of Na^+ in the bath by the impermeable cation NMDG had only a minor effect on the inward current reducing it to −4.3 ± 1 pA ($n = 103$). However, the inward current markedly increased 2.7 ± 0.1 min ($n = 103$) after changing to a hyperosmolar bath solution containing 100 mM sucrose. Osmotic cell shrinkage always preceded current activation. On average cell diameter decreased from 16.4 ± 0.2 μm under control conditions to 12.2 ± 0.2 μm in the presence of 100 mM sucrose ($n = 100$). As described previously [20, 54] and as shown in the inset of Fig. 1*A* it was possible to resolve single-channel current transitions during the initial period of whole-cell current stimulation. The single-channel conductance averaged 25.9 ± 0.9 pS ($n = 11$) which is in good agreement with values previously reported for the NSC channel in M-1 cells [25, 54]. After 6.7 ± 0.3 min ($n = 103$) the inward current reached a maximum value of 211 ± 10 pA ($n = 103$). Replacement of Na^+ with NMDG completely abolished the stimulated inward current and resulted in a small outward current (Fig. 1*A*). Under the given experimental conditions these findings indicate that the stimulated current was carried by Na^+. After washout of sucrose the cell diameter returned to 14.9 ± 0.4 μm ($n = 40$) and whole-cell currents recovered to −29 ± 15 pA ($n = 40$).

Figure 1*B* shows an experiment in which a hypo-osmolar pipette solution (200 mosmol/l) was used. The initial bath solution had the same ionic composition as the pipette solution but contained in addition 100 mM sucrose to give an osmolarity of 300 mosmol/l. The imposed osmotic gradient resulted in cell shrinkage from 12.3 ± 1.3 μm to 10.7 ± 1.2 μm ($n = 3$) and a similar current activation as previously observed with a 300 mosmol/l pipette solution and a 400 mosmol/l bath so-

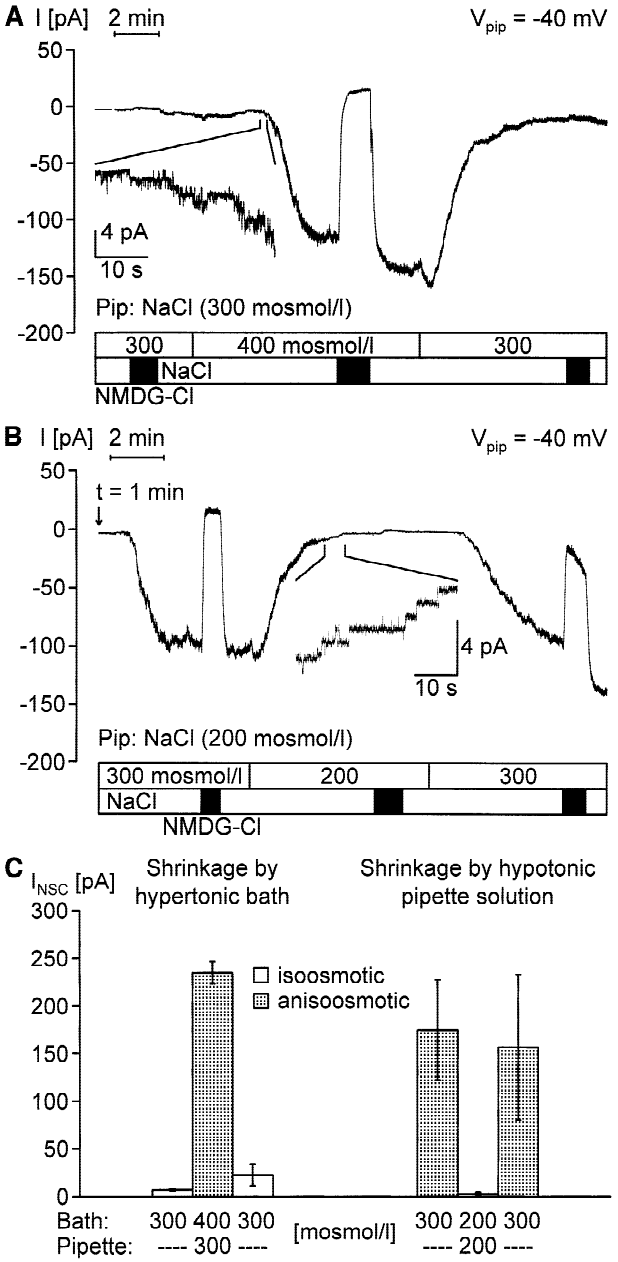

Fig. 1. Cell shrinkage by extracellular hyperosmolarity or intracellular hypo-osmolarity activates a whole-cell current in M-1 cells. Continuous whole-cell current recordings were performed at $V_{pip} = -40$ mV. Bath NaCl was periodically replaced by NMDG-Cl (lower bars) to monitor the NMDG-sensitive portion of the whole-cell current (I_{NSC}). (*A*) Bath osmolarity was increased from 300 to 400 mosmol/l by addition of 100 mM sucrose as indicated (upper bar). The NaCl pipette solution had an osmolarity of 300 mosmol/l. A portion of the current trace is expanded to demonstrate the presence of single channels. (*B*) Bath osmolarity was reduced from 300 mosmol/l to 200 mosmol/l by removing 100 mM sucrose (upper bar) while maintaining the ionic composition of the bath solution constant. The osmolarity of the NaCl pipette solution was 200 mosmol/l. (*C*) Summary of data from experiments as shown in *A* (left group of bars; $n = 103$) and *B* (right group; $n = 3$). The average I_{NSC} values are given for the various conditions. Vertical bars indicate SEM values.

lution (Fig. 1*A*). A second current activation could be elicited following re-exposure to a bath solution with an osmolarity of 300 mosmol/l. Figure 1*C* summarizes the effects of extracellular hyperosmolarity and intracellular hypo-osmolarity. On average, extracellular hyperosmolarity (bath 400 mosmol/l, pipette 300 mosmol/l) reversibly increased the NMDG-sensitive current component from 6.7 ± 1.2 pA to 235 ± 12 pA ($n = 103$). Similarly, intracellular hypo-osmolarity (bath 300 mosmol/l, pipette 200 mosmol/l) resulted in NMDG sensitive whole-cell currents that averaged 175 ± 53 pA and returned to 2.3 ± 1.5 pA ($n = 3$) upon exposure to a 200 mosmol/l bath solution. Taken together, the experiments shown in Fig. 1 demonstrate that current activation was not dependent on the presence of high extracellular osmolarity *per se* but that the osmotic gradient across the cell membrane and the resulting osmotic cell shrinkage are essential for current activation.

Selectivity of the Stimulated Whole Cell Current

Figure 2 shows individual current traces and corresponding average current/voltage (*I/V*) plots from voltage-step protocols applied during similar experiments as shown in Fig. 1*A*. The stimulated currents did not exhibit pronounced voltage-dependent activation or inactivation when voltage pulses of 400 msec duration were applied between −120 and 120 mV (Fig. 2*A*). However, the average *I/V* relationship of the stimulated current (Fig. 2*B*) was slightly outwardly rectifying. This suggests that the underlying channels have a slightly higher open probability at depolarizing voltages which is a characteristic feature of nonselective cation channels [25]. Under stimulated conditions replacement of extracellular Na^+ with NMDG shifted the reversal potential to the left (Fig. 2*B*). Measurements in zero current clamp mode revealed an average shift of the reversal potential from −4.2 ± 0.3 mV to −63 ± 1.3 mV ($n = 103$). This is consistent with the observation of a small outward current in the presence of NMDG at a holding potential of −40 mV (Fig. 1) and indicates that the stimulated channels are highly selective for cations over anions with a cation-to-anion permeability ratio of about 14. The cation selectivity of the stimulated whole-cell current was further investigated in experiments as shown in Fig. 3*A*. During maximal stimulation of whole-cell currents in hyperosmolar solution (bath solution with 100 mM sucrose) bath Na^+ was replaced by the monovalent cations K^+, Li^+ or NH_4^+. As shown before, Na^+ replacement by NMDG completely abolished the inward current under these conditions whereas replacement by K^+ or Li^+ only slightly reduced the inward currents. In the presence of NH_4^+ the

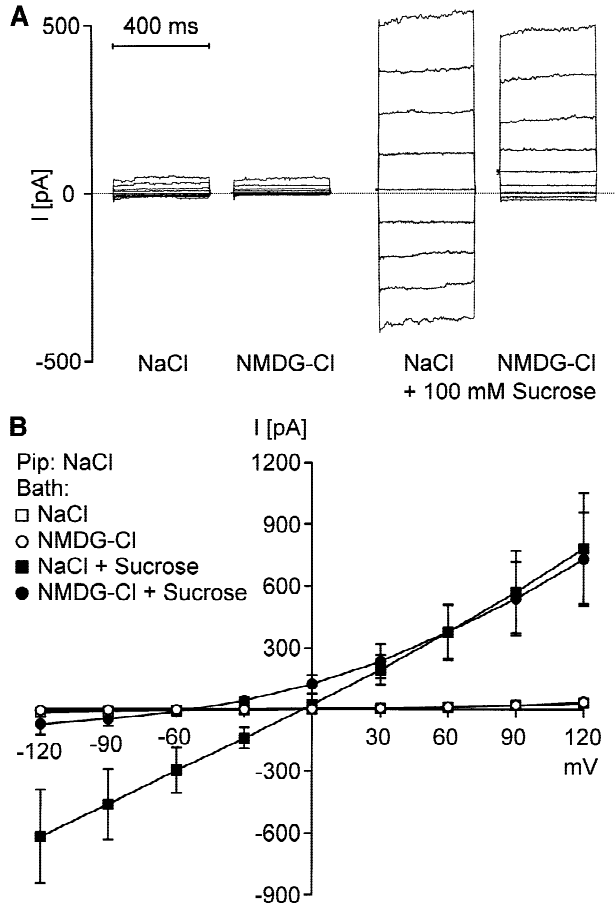

Fig. 2. (*A*) Individual whole-cell current traces obtained in M-1 cells from voltage-step protocols in the presence and absence of extracellular NaCl (replaced by NMDG-Cl) before and after changing to a hyperosmolar bath solution (+100 mM sucrose). From a holding potential (V_{pip}) of 0 mV voltage pulses of 400 msec duration were applied between −120 and +120 mV (in 30 mV increments). The pipette was filled with NaCl pipette solution. (*B*) Corresponding average *I/V* plots are shown from five similar experiments as depicted in *A*. Open symbols represent currents under iso-osmotic conditions, whereas filled symbols depict currents in hyperosmotic bath solution (+100 mM sucrose). Squares and circles indicate NaCl and NMDG-Cl containing bath solutions, respectively. Vertical bars indicate SEM values.

inward current was slightly larger than in the presence of Na^+ (Fig. 3*A*). Results from similar experiments are summarized in Fig. 3*B* and indicate a permeability sequence of NH_4^+ (1.2) ≥ Na^+ (1) ≈ K^+ (0.9) ≈ Li^+ (0.9). Hence, the stimulated channel discriminates poorly between monovalent cations.

Permeability for Divalent Cations

Nonselective cation channels may be permeable for divalent cations. Therefore we performed experiments in

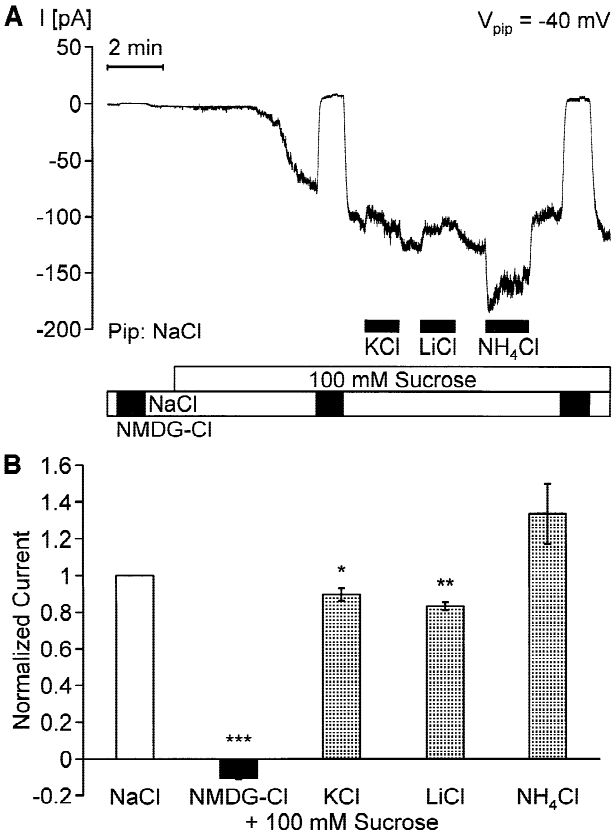

Fig. 3. Monovalent cation selectivity of shrinkage-activated whole-cell current in M-1 cells. (*A*) Experimental conditions were the same as in Fig. 1*A*. During maximal current activation after addition of 100 mM sucrose extracellular NaCl was replaced by NMDG-Cl, KCl, LiCl, or NH_4Cl. (*B*) Bar diagram summarizing results from five similar experiments as shown in *A* (LiCl and NH_4Cl: four experiments). In each experiment currents were normalized to the hyperosmolarity-activated current in the presence of NaCl. SEM values (vertical error bars) and significance levels (*$P < 0.05$, **$P < 0.01$, ***$P < 0.001$) are indicated.

which extracellular NaCl was replaced with 75 mM $CaCl_2$ or $BaCl_2$ during maximal hyperosmolar stimulation. Calcium-activated Cl^- channels are known to be present in M-1 cells [34] and preliminary experiments indicated that with a standard pipette solution containing 1 mM EGTA a change of the bath solution to 75 mM $CaCl_2$ raised the subplasmalemmal calcium sufficiently to activate these channels ($n = 4$, *data not shown*). To prevent interference from calcium-activated Cl^- channels we used pipette solutions containing either 10 mM EGTA or 10 mM BAPTA. A typical experiment with 10 mM BAPTA in the pipette solution is shown in Fig. 4*A*. During hyperosmolar stimulation replacement of bath Na^+ with Ca^{2+} had a similar effect on the whole cell current as Na^+ replacement with the impermeant cation NMDG. At a holding potential of −40 mV no inward current was

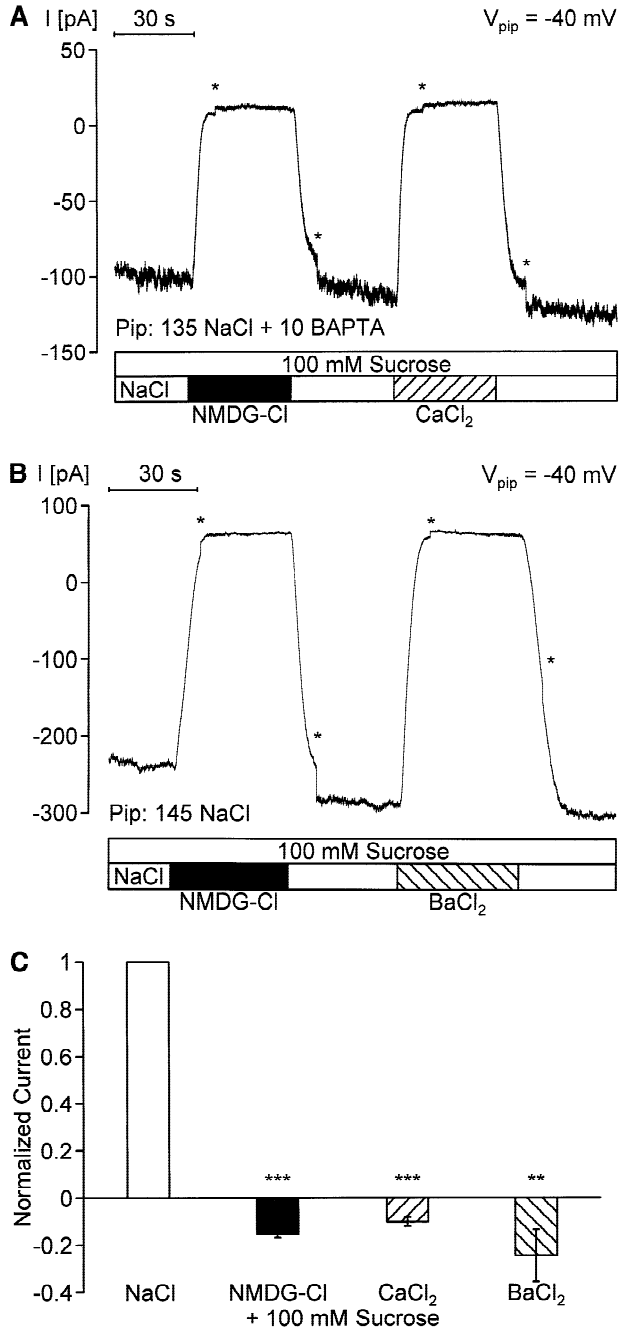

Fig. 4. Divalent cation selectivity of shrinkage-activated whole-cell current in M-1 cells. Continuous whole-cell current recordings were performed at $V_{pip} = -40$ mV. Asterisks indicate correction of the holding potential to compensate liquid junction potentials. During maximal current activation after addition of 100 mM sucrose the extracellular NaCl was replaced by NMDG-Cl (for comparison) and subsequently by $CaCl_2$ (*A*) or $BaCl_2$ (*B*). In the experiment shown in *A* the pipette contained 10 mM BAPTA. (*C*) Summary of results from several experiments as depicted in *A* and *B*. The shrinkage-activated whole-cell currents in the presence of NMDG-Cl ($n = 7$), $CaCl_2$ ($n = 4$), and $BaCl_2$ ($n = 3$) are normalized to the current in the presence of NaCl.

detectable in the presence of 75 mM Ca^{2+} in the bath solution. This is consistent with a change of the reversal potential from −0.3 ± 0.6 mV to −63.8 ± 3.5 mV (n = 9) indicating a Na^+ to Ca^{2+} permeability ratio >100. As shown in Fig. 4*B*, replacement of bath Na^+ with 75 mM Ba^{2+} had a similar effect. Again there were no Ba^{2+} inward currents detectable and the reversal potential changed from −4.2 ± 1.9 to −80.9 ± 9.2 (n = 3) indicating a Na^+ to Ba^{2+} permeability ratio of >100. Results from similar experiments are summarized in Fig. 4*C*.

Role of Intracellular Ca^{2+}

The NSC channel in inside-out patches of M-1 cells is activated by cytosolic Ca^{2+} at a threshold of about 1 μM [25]. However, as previously shown, shrinkage-induced activation of the NSC channel is largely independent of intracellular and extracellular calcium [54]. This is consistent with the findings of the present study in which activation of NSC currents by cell shrinkage was preserved in M-1 cells dialyzed with Ca^{2+}-free pipette solutions containing high concentrations of calcium chelators (Fig. 4*A*). With 10 mM EGTA or 10 mM BAPTA in the pipette solution and holding at a potential of −40 mV, cell shrinkage stimulated NMDG-sensitive NSC currents which averaged 160 ± 23.6 pA (n = 7) and 94.4 ± 42.1 pA (n = 6), respectively. Interestingly, in the presence of 10 mM BAPTA, but not 10 mM EGTA, the stimulated current was significantly smaller than under control conditions with 1 mM EGTA in the pipette solution (235 ± 12 pA, n = 103, Fig. 1*C*; $P < 0.05$). This may indicate that BAPTA in high concentrations may have a nonspecific inhibitory effect or that chelating intracellular calcium below a critical level may ultimately interfere with the activation mechanism of the NSC channel.

Effect of Drugs

The effects of a number of putative inhibitory drugs on the shrinkage-activated whole-cell current during maximal stimulation are summarized in Fig. 5. Ca^{2+}-activated, ATP-sensitive NSC channels in many tissues are typically inhibited by derivatives of diphenylamine-2-carboxylic acid (DPC) [7, 10, 11, 18, 22, 43, 46]. Flufenamic acid (100 μM) reduced the shrinkage-activated inward currents by approximately 83% (Fig. 5) which is consistent with our previous findings [20, 54]. Two other DPC-derivatives, DCDPC and 4-methyl-DPC, were similarly effective with an average inhibitory effect of 75 and 79%, respectively. The isoquinoline derivative LOE 908, which inhibits nonselective cation channels in A7r5 vascular smooth muscle cells with an IC50 of 560 nM [26], inhibited the shrinkage-activated NSC inward current by 49% when applied at a concentration of 10 μM. Amiloride is a potent blocker of the epithelial sodium channel (ENaC) and has also been shown to inhibit nonselective cation channels in rat medullary collecting duct cells [30], while bumetanide specifically inhibits the $Na^+/K^+/2Cl^-$ transport known to be activated during cell shrinkage [40]. However, application of amiloride (1 mM) had only a minor effect while bumetanide (30 μM) was ineffective (Fig. 5). Taken together our findings suggest that ENaC and the $Na^+/K^+/2Cl^-$ transporter are not involved in the current activation observed upon cell shrinkage. At present flufenamic acid is probably the most useful inhibitor of the shrinkage-activated NSC channel. However, its usefulness is compromised by the fact that relatively high concentrations (100 μM) of flufenamic acid are needed. Moreover, flufenamic acid has been reported to cause Ca^{2+} release from intracellular stores [44], may act as a mitochondrial uncoupler [33], and also inhibits various chloride channels, e.g. swelling-activated Cl^- channels in M-1 cells [34].

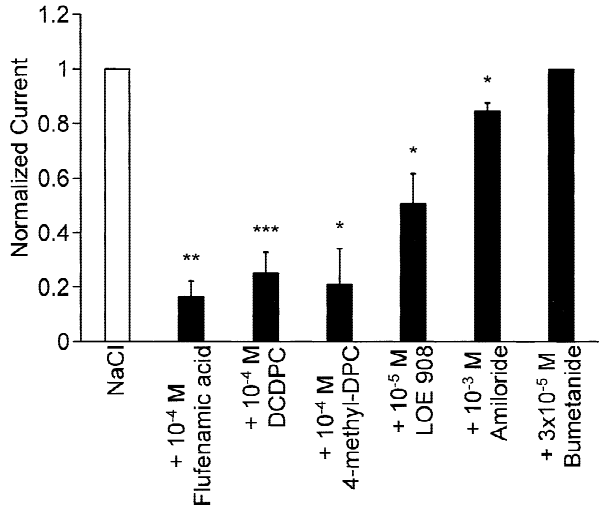

Fig. 5. Effect of inhibitors on the shrinkage-activated whole-cell conductance of M-1 cells. During maximal whole-cell current activation by addition of 100 mM sucrose the effect of various inhibitors was tested. Currents are normalized to the inward currents measured in the presence of NaCl and 100 mM sucrose prior to the addition of the drug (DCDPC: n = 5; amiloride: n = 4; flufenamic acid, 4-methyl-DPC, LOE 908, and bumetanide: n = 3). Experimental conditions were the same as in Fig. 1*A*.

We also investigated the effect of maitotoxin (MTX) on whole-cell currents of M-1 cells. Maitotoxin is a potent marine toxin which has been shown to activate nonselective cation channels in a variety of cell types. A 1-min application of 1 nM MTX has been shown to activate a nonselective cation conductance in *Xenopus laevis* oocytes increasing the NMDG-sensitive currents more than 100-fold [2]. Despite this, application of 1 nM MTX failed to elicit a significant whole-cell current response in M-1 cells whereas subsequent exposure to extracellular hyperosmolarity had the usual stimulatory ef-

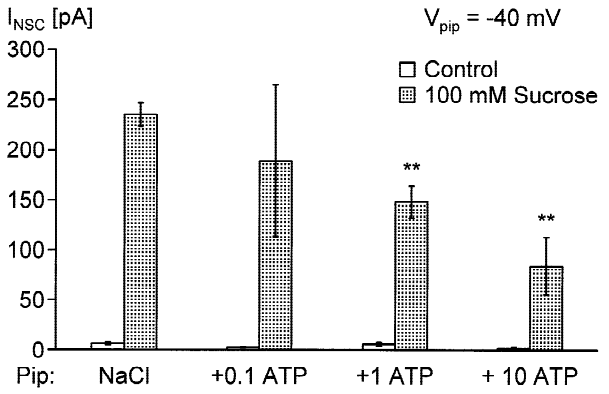

Fig. 6. Intracellular ATP reduces the whole-cell current response to cell shrinkage in a concentration-dependent manner. Whole-cell currents were activated by addition of 100 mM sucrose as shown in Fig. 1*A*. In the bar diagram the NMDG-sensitive whole-cell currents (I_{NSC}) are shown before and after current activation by 100 mM sucrose using pipette solutions which contained either no ATP (NaCl: $n = 103$) or ATP in the concentrations indicated (0.1 mM: $n = 6$; 1 mM: $n = 5$; 10 mM: $n = 6$).

fect ($n = 5$). Accordingly, the shrinkage-activated NSC does not seem to be affected by MTX.

ATP Dependence of the Whole-Cell Current Activation by Cell Shrinkage

In excised inside-out patches the NSC channel of M-1 cells is largely inhibited by millimolar concentrations of ATP or ADP [25]. As shown in Fig. 6, in the presence of 1 or 10 mM ATP in the pipette solution the magnitude of the shrinkage-activated NSC currents was significantly reduced by 39 or 65%, respectively. However, the qualitative response was preserved even in the presence of 10 mM ATP which is consistent with previous findings [54]. Therefore, intracellular ATP concentrations within the physiological range do not prevent shrinkage-activation of NSC channels.

On the other hand, an ATP dependence of the activation mechanism of swelling-activated Cl^- channels has been demonstrated in a variety of cell types including M-1 cells [34]. Therefore, in the present study the ATP dependence of the whole-cell current response to hyperosmolar cell shrinkage was investigated. To this end ATP-depleted cells were kept in the continuous presence of 100 nM rotenone (or 2.5 μM FCCP) and 5 mM 2-deoxyglucose. These drugs were added to the pipette and bath solutions which contained no glucose (*see* Materials and Methods). In ATP-depleted cells dialyzed with an ATP-free pipette solution, the usual increase of the NMDG-sensitive whole-cell current in response to osmotic cell shrinkage was almost completely absent. Results of rotenone-treated cells (Fig. 7*A*) were similar to those of cells treated with FCCP (Fig. 7*B*). Supplementing the pipette solution with 0.1 or 1 mM ATP did not restore the whole-cell current response in ATP-depleted cells. This indicates that ATP-depletion had a prolonged inhibitory effect on the shrinkage activation of the NSC channel which could not be overcome by the acute re-addition of ATP. To test whether a prolonged recovery period would restore the current response to cell shrinkage, ATP-depleted cells were rinsed with rotenone-free (FCCP-free) NaCl bath solution and subsequently maintained in PC-1 tissue culture medium at 37°C/5% CO_2 for 1–3 hours. After this recovery period the current response to osmotic cell shrinkage was fully restored (Fig. 7).

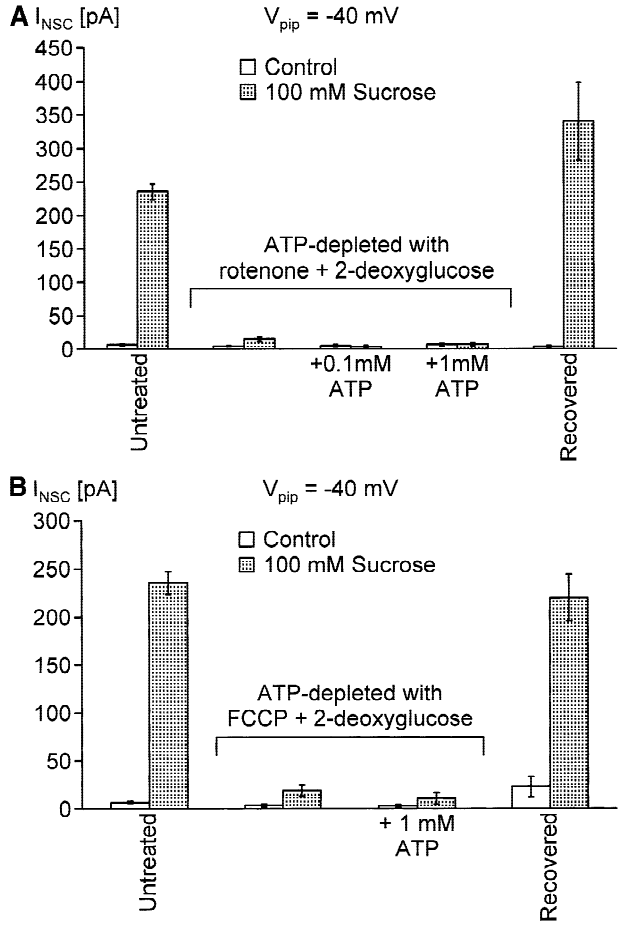

Fig. 7. ATP-depletion inhibits activation of whole-cell currents by cell shrinkage. ATP-depletion was achieved in the presence of 2 mM 2-deoxyglucose by using 100 nM rotenone (*A*) or 2.5 μM FCCP (*B*). Whole-cell currents were stimulated by addition of 100 mM sucrose using the experimental conditions as in Fig. 1*A*. NMDG-sensitive whole-cell currents (I_{NSC}) were measured before and after current activation by 100 mM sucrose in untreated control cells (same set of data as shown in Fig. 6; $n = 103$), in ATP-depleted cells (*A:* $n = 12$; *B:* $n = 9$), and in cells that were allowed to recover from ATP-depletion (*A:* $n = 6$; *B:* $n = 4$). In some experiments the pipette solution was supplemented with 0.1 mM (*A:* $n = 4$) or 1 mM ATP (*A:* $n = 8$; *B:* $n = 9$) to test the acute reversibility of ATP-depletion.

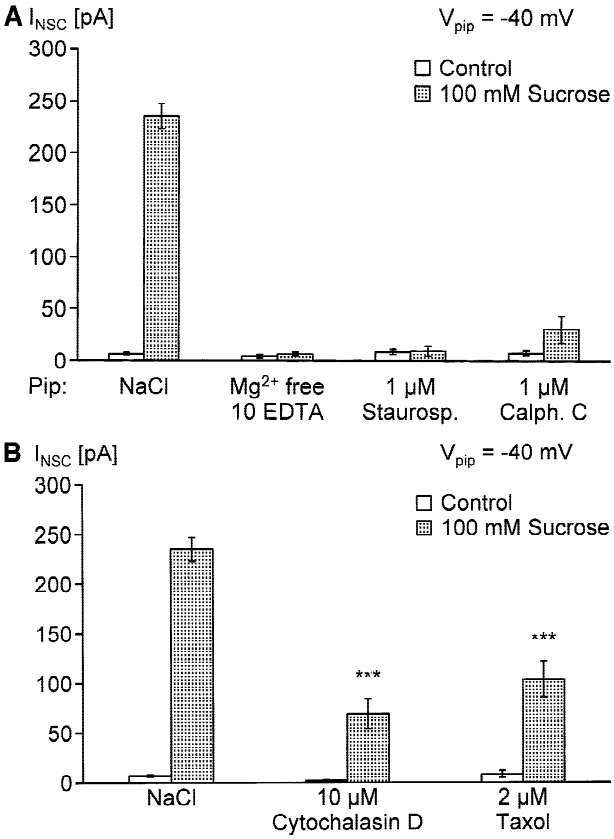

Fig. 8. (*A*) Shrinkage activation is dependent on intracellular Mg^{2+} and is inhibited by protein kinase inhibitors. Mg^{2+}-free pipette solution contained 10 mM EDTA to minimize intracellular free Mg^{2+} concentration ($n = 7$). Cells were pretreated with 1 μM staurosporine ($n = 8$) or 1 μM calphostin C ($n = 9$) for about 60 min. Inhibitors were also added to the standard NaCl pipette solution. (*B*) Inhibitory effect of cytochalasin D and taxol. Cells were pretreated for 45–60 min using cytochalasin D ($n = 10$) and taxol ($n = 9$) in concentrations of 10 and 2 μM. The inhibitors were also included in the pipette. NMDG-sensitive whole-cell currents (I_{NSC}) were measured before and after current activation by 100 mM sucrose. Values obtained in untreated control cells (NaCl) are given for comparison (same set of data as shown in Fig. 6; $n = 103$).

Mg^{2+} Dependence and Effects of Kinase Inhibitors and Drugs Interfering with the Cytoskeleton

The ATP-dependence of the current activation in response to cell shrinkage suggested that a protein kinase reaction may be involved in the activation mechanism. Kinase reactions are usually Mg^{2+}-dependent. As shown in Fig. 8*A* shrinkage-activated NSC currents were not observed in cells dialyzed with Mg^{2+}-free pipette solution containing 10 mM EDTA. This indicates that an enzymatic reaction requiring magnesium as a cofactor may be involved. We also tested the effects of the kinase inhibitors staurosporine and calphostin C. Cells were pretreated with 1 μM staurosporine or 1 μM calphostin C for about an hour and the kinase inhibitors were also included in the pipette solution. As shown in Fig. 8*A* the current stimulation by cell shrinkage was largely inhibited by both staurosporine and calphostin C. These experiments suggest the involvement of a protein kinase in the activation mechanism.

To investigate the possible role of an intact cytoskeleton for the shrinkage-activated current response experiments were performed using cytochalasin D, a substance known to prevent both association and dissociation of F-actin subunits from filaments [8], or taxol, which supports polymerization of microtubules [38]. A 45–60 min preincubation in 10 μM cytochalasin D or 2 μM taxol significantly reduced the magnitude of the current response to cell shrinkage (Fig. 8*B*) consistent with a role of the cytoskeleton in the activation mechanism.

Discussion

In the present study we confirmed that the shrinkage-activated channels discriminate poorly between monovalent cations. In contrast, we found that they have no measurable conductance for Ca^{2+} or Ba^{2+} which distinguishes them from calcium-permeable nonselective cation channels described in other preparations. Derivatives of diphenylamine-2-carboxylic acid (DPC) such as flufenamic acid were the most effective channel blocking agents among various drugs tested, while maitotoxin, a putative NSC channel opener, had no effect.

This study also provides new insight regarding the mechanism of channel activation. Using pipette solutions with reduced osmolarity to shrink the cells, we were able to demonstrate that extracellular hyperosmolarity *per se* is not required for channel activation and that cell shrinkage is the activating trigger. This indicates that no specific sensor for extracellular osmolarity is involved in the activation mechanism. Furthermore, in the whole-cell configuration a major rise in intracellular calcium concentration ($[Ca^{2+}]_i$) does not seem to be necessary for shrinkage-induced channel activation, which is in contrast to the calcium-dependence of channel activation in inside-out patches. However, buffering $[Ca^{2+}]_i$ with high concentrations of EGTA or BAPTA (10 mM) slightly reduced the magnitude of the shrinkage-induced response. This suggests that reducing $[Ca^{2+}]_i$ to very low levels eventually interferes with components of the signal transduction mechanism involved.

Possibly the most intriguing finding of the present study is the dual effect of ATP where high concentrations of intracellular ATP reduced the magnitude of shrinkage-activation consistent with ATP's inhibitory effect in inside-out patches, while ATP depletion of the cells completely abolished shrinkage-activation. This indicates that in addition to its inhibitory effect ATP is essential for channel activation. Interestingly, the ab-

sence of intracellular Mg^{2+} which is required for many kinase-mediated reactions, or pretreatment with the kinase inhibitors staurosporine and calphostin C largely suppressed the stimulatory response to cell shrinkage. In addition it was shown that modifying the cytoskeleton with cytochalasin D and taxol also had an inhibitory effect. Taken together, these findings suggest that phosphorylation steps and ATP-dependent cytoskeletal elements are involved in NSC channel activation by cell shrinkage.

Selectivity of the Shrinkage-Activated Conductance

The shrinkage-activated conductance discriminates poorly between monovalent cations with a selectivity sequence NH_4 (1.2) $\geq$ Na^+ (1) $\approx$ K^+ (0.9) $\approx$ Li^+ (0.9). On the other hand the channel is highly selective for cations over anions with a permeability ratio of about 14.

Calcium-permeable nonselective cation channels may constitute important entry pathways for extracellular Ca^{2+}, for example I_{CRAC} channels [41] or members of the *trp/trpl* family of ion channels originally cloned from *Drosophila* [53] and also found in mammalian tissues [59]. However, our study shows that the shrinkage-activated NSC channels in M-1 cells have no measurable macroscopic conductance for divalent cations which is consistent with previous single-channel data from excised inside-out patches [25]. Nevertheless, a very small Ca^{2+} permeability with a single channel Ca^{2+} conductance in the sub-pS range cannot be ruled out at present and may be responsible for the occasional activation of putative Ca^{2+}-activated Cl^- channels during hyperosmolar shrinkage in the presence of high extracellular calcium using a pipette solution containing only 1 mM EGTA (*data not shown*). This may be due to a minimal calcium permeability of the activated NSC channels but may also be the result of a shrinkage induced deterioration of the 'seal' resistance favoring a calcium leak via the 'seal'. In any case, the absence of measurable divalent membrane whole-cell currents demonstrates that the shrinkage-activated NSC is different from highly calcium-permeable nonselective cation channels described in various preparations. Thus, the shrinkage-activated NSC channel is unlikely to serve as a Ca^{2+} entry pathway under physiological conditions including cell shrinkage.

Physiological Intracellular Calcium Levels are Sufficient for Shrinkage-Activation of NSC Channels

In excised inside-out patches of M-1 cells the NSC channel is known to be activated by cytoplasmic calcium at a threshold of 10^{-6} M with near maximal activation at 10^{-3} M [25]. Such high intracellular calcium levels are unlikely to be reached under physiological conditions. In our whole-cell experiments a major role of Ca^{2+} as signal for shrinkage-activation was essentially ruled out, since channel activation was preserved in experiments with nominally calcium-free pipette solution containing 10 mM EGTA which is consistent with our previous findings [54]. As demonstrated in the present study, shrinkage-activation of the NSC channel was observed even in the presence of the strong Ca^{2+} chelator BAPTA (10 mM) in the pipette solution. This is in good agreement with the view that $[Ca^{2+}]_i$ signaling plays an important role for volume regulation during hypo-osmolar cell swelling, but is less important during hyperosmolar shrinkage [32]. However, it was noticed that the stimulatory responses were somewhat attenuated with 10 mM EGTA and 10 mM BAPTA in the pipette solution compared to the response with standard pipette solution containing only 1 mM EGTA. Hence, a minimal level of intracellular or subplasmalemmal free Ca^{2+} appears to be required for the activation mechanism possibly involving Ca^{2+}-sensitive regulatory or structural proteins. It is likely that a complex regulatory machinery responsible for shrinkage-activation includes a number of channel-associated proteins and soluble cytosolic factors. Disruption of the cytoskeleton by patch excision and loss of some of the regulatory components could change the calcium-sensitivity of the channel (*see below*). This may explain why full channel activation in excised inside-out patches requires cytosolic calcium concentrations in the millimolar range. In any case, the findings of the present study suggest that in an intact cell the intracellular calcium levels required for shrinkage-activation of the NSC channel are not above the normal physiological range.

Dual Effect of ATP

Most Ca^{2+}-activated NSC channels have been found to be inhibited by high cytosolic ATP concentrations in excised inside-out patches [45]. In M-1 cells 1 mM cytosolic ATP caused a reduction of approximately 70% of the open probability of NSC channels studied in excised inside-out patches [25]. In whole-cell recordings 1 mM ATP in the pipette solution appeared to be slightly less efficient inhibiting the shrinkage-activation of the NSC channel on average by about 40% (Fig. 6). This may be due to partial intracellular ATP breakdown resulting in a less than 1 mM subplasmalemmal ATP concentration. Indeed, the inhibitory effect was more pronounced with 10 mM ATP in the pipette solution averaging approximately 70% which is in good agreement with the degree of inhibition reported previously [54]. The inhibitory effect of ATP on the shrinkage-activation was concentration-dependent and consistent with the inhibitory effect of ATP on NSC channel activity in excised inside-out patches. However, even with 10 mM ATP in the pipette

solution a substantial shrinkage-activation of the NSC channel was preserved. Thus, physiological cytosolic ATP levels are unlikely to prevent a shrinkage-activation of the NSC channel.

On the other hand, the ATP-depletion experiments demonstrated that the presence of cytosolic ATP was essential for channel action. When formation of intracellular ATP was inhibited, cell shrinkage no longer elicited a stimulatory response. Interestingly, in ATP-depleted cells acute ATP repletion by including ATP in the pipette solution did not restore the shrinkage-activated response. In contrast, in similar experiments ATP repletion of M-1 cells via the pipette solution immediately restored Cl^- channel activation in response to hypo-osmolar cell swelling [34]. When cells were allowed to recover from ATP-depletion in tissue culture medium for an extended period of time, shrinkage-activation of the NSC channel was again observed. The delayed recovery from ATP-depletion suggests that the role of ATP for channel activation is complex and probably involves more than a direct interaction of ATP with a putative ATP-binding site of the channel.

Our finding of a dual effect of ATP, which inhibits but is also essential for channel activation, is reminiscent of the dual effect of ATP on the apical small conductance K^+ channel of rat cortical collecting duct where low concentrations of ATP are required as a substrate for protein kinase A to activate the channel whereas millimolar concentrations of ATP reduce channel open probability [57]. The physiological role of the ATP regulation of this renal K^+ secretory channel, which is believed to correspond to the cloned ROMK channel, is not completely understood. However, there is recent evidence that the complex effects of ATP on channel activity may be mediated by additional associated proteins [56]. This further supports our interpretation that the activation mechanism of the shrinkage-activated NSC channel is complex and probably involves more than a phosphorylation of the channel itself.

Possible Involvement of Protein Kinases

The Mg^{2+} dependence of the shrinkage-activation and the inhibitory effect of kinase inhibitors suggest that intracellular ATP is essential for phosphorylation steps involved in the activation mechanism of the NSC channel. Mitogen-activated protein (MAP) kinases [9, 14], and a serine/threonine protein kinase [55] have been cloned that are activated by extracellular hyperosmolarity. Moreover, protein-tyrosine kinases may play a role in the signaling of hyperosmotic shock [27, 51]. Recently, cell shrinkage has been shown to specifically activate the *fyn* kinase, a member of the *src* family, and to induce tyrosine phosphorylation of cortactin thought to be involved in the organization of the cortical actin skeleton [19]. Interestingly, cell shrinkage and not an increase in the extracellular osmolarity or intracellular ion composition was shown to be the signal that elicited protein tyrosine phosphorylation [27, 51]. These findings imply that cells detect alterations in cell size rather than changes in osmolarity or ionic strength. This is consistent with our finding that the NSC channels did not respond to extracellular osmolarity *per se* but to cell shrinkage.

Staurosporine is a rather nonspecific protein kinase inhibitor while calphostin C is believed to have a relatively high specificity for protein kinase C [52]. However, the concentrations used in the present study were rather high (μM) and inhibition of the protein kinase C pathway may have downstream effects on the MAP kinase pathway. Thus, additional studies are necessary to identify the protein kinases involved in the shrinkage-induced activation of the NSC channel. Highly specific protein kinase inhibitors would be needed but are not readily available at present. However, the present study strongly suggests that Mg^{2+}-dependent protein phosphorylation is involved in the activation of the NSC channel by cell shrinkage.

Possible Role of the Cytoskeleton

Cytoskeletal elements are obvious candidates to be involved in shrinkage-activation of ion channels and may serve as sensors in the signal transduction pathway [16]. Indeed, the inhibitory effect of cytochalasin D observed in the present study suggests that an intact actin system is essential for shrinkage-activated NSC channel activation. Since ATP depletion has been shown to destabilize the actin filament network and to cause a cellular redistribution of the cortical F-actin cytoskeleton [12, 36] the inhibitory effect of ATP depletion is consistent with an involvement of actin in NSC channel activation. Interestingly, it has been reported that cell shrinkage itself also triggers changes in the actin filament network leading to an increase in cellular F-actin content [42]. There are several examples of ion channels that are modulated in their function by actin filaments [4, 5, 50]. The inhibitory effect of ATP-depletion observed in the present study is compatible with an involvement of actin filaments or other ATP-dependent cytoskeletal components in the shrinkage-activation of the NSC channel. Interestingly, disruption of the microtubule turnover with taxol also decreased shrinkage-induced activation of NSC channel currents. The ATP-dependent 'microtubule motors' may play a role for ion channel trafficking and insertion into the plasma membrane [16] and an intact microtubule system may be necessary for shrinkage-activation of NSC channels. The involvement of actin and the cytoskeleton is consistent with the finding that the inhibitory effect of ATP-depletion was not im-

mediately reversible. It may also explain the different sensitivities for Ca^{2+} and ATP in the whole cell and inside out-configuration, since patch excision is likely to disrupt the intimate connections between the plasma membrane and cytoskeletal elements [35].

Possible Physiological Significance

Activation of the NSC channel by cell shrinkage suggests that this channel plays a role in regulating the cell volume. It is well established that cell shrinkage activates $Na^+/K^+/2Cl^-$ cotransport and Na^+/H^+ antiport which are both believed to contribute to solute accumulation during regulatory volume increase [40]. In addition shrinkage-activated Na^+ channels or NSC channels may be involved [6, 54, 58]. The opening of these channels leads to Na^+ uptake and depolarization of the cell. An effective Na^+ uptake leading to a rise in intracellular osmolarity with subsequent water uptake relies on a parallel anion uptake. Under the experimental conditions of this study no shrinkage-activated Cl^- conductance was observed, but the intrinsic Cl^- conductance of the cells is probably sufficient to facilitate a conductive Cl^- inward flux at rising cell potentials. As a further step the rise in intracellular Na^+ concentration could lead to activation of the Na^+/K^+-ATPase with a following rise of intracellular K^+ content. Apart from this, the Na^+ inward current and parallel depolarization of the cell could possibly activate or modulate signal transduction pathways such as MAP kinases. In this context it is interesting to note that intracellular receptors for Na^+ may exist [23] and may sense a rise in intracellular Na^+ concentration as a first step in a complex signaling cascade.

Finally, high extracellular osmolarity can cause apoptosis which is known to accompany cell shrinkage [3, 31]. How cell volume changes and how volume regulatory mechanisms are involved in programmed cell death is not yet clear [28]. However, ion channels are thought to play a role in the induction of apoptosis [1, 37]. Moreover, sodium overload through voltage-dependent Na^+ channels has recently been shown to induce apoptosis in rat cervical ganglion cells [21]. Thus, if cell shrinkage is an essential step in apoptosis, the shrinkage-activated NSC channel should be involved in the apoptotic process. Such a role would be consistent with the ubiquitous but normally quiescent presence of NSC channels in a large variety of cells. Moreover, since mitochondrial membrane permeabilization occurs during apoptosis [15] the expected decline of intracellular ATP would favor the activation of the shrinkage-activated NSC channels under apoptotic conditions.

The expert technical assistance of U. Fink and I. Doering-Hirsch is gratefully acknowledged. We thank Dr. B. Letz and A. Rabe for programming the computer software. This work was supported by a grant from the Deutsche Forschungsgemeinschaft (DFG grant Fr 233/9-1 and Ko 1057/7-1) and the Wellcome Trust. The authors thank Prof. Dr. E. Frömter for helpful discussions.

References

1. Beauvais, F., Michel, L., Dubertret, L. 1995. Human eosinophils in culture undergo a striking and rapid shrinkage during apoptosis. Role of K^+ channels. *J. Leuk. Biol.* **57:**851–855
2. Bielfeld-Ackermann, A., Range, C., Korbmacher, C. 1998. Maitotoxin (MTX) activates a nonselective cation channel in *Xenopus laevis* oocytes. *Pfluegers Arch.* **436:**329–337
3. Bortner, C.D., Cidlowski, J.A. 1996. Absence of volume regulatory mechanisms contributes to the rapid activation of apoptosis in thymocytes. *Am. J. Physiol.* **271:**C950–C961
4. Cantiello, H.F. 1995. Role of the actin cytoskeleton on epithelial Na^+ channel regulation. *Kidney Int.* **48:**970–984
5. Cantiello, H.F., Stow, J.L., Prat, A.G., Ausiello, D.A. 1991. Actin filaments regulate epithelial Na^+ channel activity. *Am. J. Physiol.* **261:**C882–C888
6. Chan, H.C., Nelson, D.J. 1992. Chloride-dependent cation conductance activated during cellular shrinkage. *Science* **257:**669–671
7. Chraïbi, A., Van den Abbeele, T., Guinamard, R., Teulon, J. 1994. A ubiquitous non-selective cation channel in the mouse renal tubule with variable sensitivity to calcium. *Pfluegers Arch.* **429:**90–97
8. Cooper, J.A. 1987. Effects of Cytochalasin and Phalloidin on Actin. *J. Cell Biol.* **105:**1473–1478
9. Galcheva Gargova, Z., Derijard, B., Wu, I.H., Davis, R.J. 1994. An osmosensing signal transduction pathway in mammalian cells. *Science* **265:**806–808
10. Gögelein, H., Dahlem, D., Englert, H.C., Lang, H.J. 1990. Flufenamic acid, mefenamic acid and niflumic acid inhibit single nonselective cation channels in the rat exocrine pancreas. *FEBS Lett.* **268:**79–82
11. Gögelein, H., Pfannmüller, B. 1989. The nonselective cation channel in the basolateral membrane of rat exocrine pancreas. *Pfluegers Arch.* **413:**287–298
12. Golenhofen, N., Doctor, R.B., Bacallao, R., Mandel, L.J. 1995. Actin and villin compartmentation during ATP depletion and recovery in renal cultured cells. *Kidney Int.* **48:**1837–1845
13. Hamill, P., Marty, A., Neher, E., Sakmann, B., Sigworth, F.J. 1981. Improved patch-clamp techniques for high-resolution current recording from cells and cell-free membrane patches. *Pfluegers Arch.* **391:**85–100
14. Han, J., Lee, J.D., Bibbs, L., Ulevitch, R.J. 1994. A MAP kinase targeted by endotoxin and hyperosmolarity in mammalian cells. *Science* **265:**808–811
15. Jacotot, E., Costantini, P., Laboureau, E., Zamzami, N., Susin, S.A., Kroemer, G. 1999. Mitochondrial membrane permeabilization during the apoptotic process. *Ann. N.Y. Acad. Sci.* **887:**18–30
16. Janmey, P.A. 1998. The cytoskeleton and cell signaling: component localization and mechanical coupling. *Physiol. Rev.* **78:**763–781
17. Jirsch, J.D., Loe, D.W., Cole, S.P., Deeley, R.G., Fedida, D. 1994. ATP is not required for anion current activated by cell swelling in multidrug-resistant lung cancer cells. *Am. J. Physiol.* **267:**C688–C699
18. Jung, F., Selvaraj, S., Gargus, J.J. 1992. Blockers of platelet-derived growth factor-activated nonselective cation channel inhibit cell proliferation. *Am. J. Physiol.* **262:**C1464–C1470
19. Kapus, A., Szaszi, K., Sun, J., Rizoli, S., Rotstein, O.D. 1999. Cell shrinkage regulates Src kinases and induces tyrosine phosphorylation of cortactin, independent of the osmotic regulation of Na^+/H^+ exchangers. *J. Biol. Chem.* **274:**8093–8102

20. Koch, J.-P., Korbmacher, C. 1999. Osmotic shrinkage activates nonselective (NSC) channels in various cell types. *J. Membrane Biol.* **168:**131–139
21. Koike, T., Ninomiya, T. 2000. Alteration of veratridine neurotoxicity in sympathetic neurons during development in vitro. *Neuroreport* **11:**151–155
22. Koivisto, A., Klinge, A., Nedergaard, J., Siemen, D. 1998. Regulation of the activity of 27 pS nonselective cation channels in excised membrane patches from rat brown fat cells. *Cell. Physiol. Biochem.* **8:**231–245
23. Komwatana, P., Dinudom, A., Young, J.A., Cook, D.I. 1998. Activators of epithelial Na^+ channels inhibit cytosolic feedback control. Evidence for the existence of a G protein-coupled receptor for cytosolic Na^+. *J. Membrane Biol.* **162:**225–232
24. Korbmacher, C., Barnstable, C.J. 1993. Renal epithelial cells show nonselective cation channel activity and express a gene related to the cGMP-gated photoreceptor channel. *In:* Nonselective Cation Channels. D. Siemen and J.K.-J. Hescheler, editors. pp. 147–164. Birkhäuser Verlag, Basel
25. Korbmacher, C., Volk, T., Segal, A.S., Boulpaep, E.L., Fromter, E. 1995. A calcium-activated and nucleotide-sensitive nonselective cation channel in M-1 mouse cortical collecting duct cells. *J. Membrane Biol.* **146:**29–45
26. Krautwurst, D., Degtiar, V.E., Schultz, G., Hescheler, J. 1994. The isoquinoline derivative LOE 908 selectively blocks vasopressin-activated nonselective cation currents in A7r5 aortic smooth muscle cells. *Naunyn-Schmied Arch. Pharmacol.* **349:**301–307
27. Krump, E., Nikitas, K., Grinstein, S. 1997. Induction of tyrosine phosphorylation and Na^+/H^+ exchanger activation during shrinkage of human neutrophils. *J. Biol. Chem.* **272:**17303–17311
28. Lang, F., Busch, G.L., Ritter, M., Völkl, H., Waldegger, S., Gulbins, E., Häussinger, D. 1998. Functional significance of cell volume regulatory mechanisms. *Physiol. Rev.* **78:**247–273
29. Letz, B., Ackermann, A., Canessa, C.M., Rossier, B.C., Korbmacher, C. 1995. Amiloride-sensitive sodium channels in confluent M-1 cortical collecting duct cells. *J. Membrane Biol.* **148:**127–141
30. Light, D.B., McCann, F., Keller, T.M., Stanton, B.A. 1988. Amiloride-sensitive cation channel in apical membrane of inner medullary collecting duct. *Am. J. Physiol.* **255:**F278–F286
31. Matthews, C.C., Feldman, E.L. 1996. Insulin-like growth factor I rescues SH-SY5Y human neuroblastoma cells from hyperosmotic induced programmed cell death. *J. Cell. Physiol.* **166:**323–331
32. McCarty, N.A., O'Neil, R.G. 1992. Calcium signaling in cell volume regulation. *Physiol. Rev.* **72:**1037–1061
33. McDougall, P., Markham, A., Cameron, I., Sweetman, A.J. 1988. Action of the nonsteroidal anti-inflammatory agent, flufenamic acid, on calcium movements in isolated mitochondria. *Biochem. Pharmacol.* **37:**1327–1330
34. Meyer, K., Korbmacher, C. 1996. Cell swelling activates ATP-dependent voltage-gated chloride channels in M-1 mouse cortical collecting duct cells. *J. Gen. Physiol.* **108:**177–193
35. Milton, R.L., Caldwell, J.H. 1990. How do patch-clamp seals form? A lipid bleb model. *Pfluegers Arch.* **416:**758–762
36. Molitoris, B.A., Dahl, R., Hosford, M. 1996. Cellular ATP depletion induces disruption of the spectrin cytoskeletal network. *Am. J. Physiol.* **271:**F790–F798
37. Nagy, P., Panyi, G., Jenei, A., Bene, L., Gáspár, R., Jr., Matkó, J., Damjanovich, S. 1995. Ion-channel activities regulate transmembrane signaling in thymocyte apoptosis and T-cell activation. *Immunol. Lett.* **44:**91–95
38. Oike, M., Schwarz, G., Sehrer, J., Jost, M., Gerke, V., Weber, K., Droogmans, G., Nilius, B. 1994. Cytoskeletal modulation of the response to mechanical stimulation in human vascular endothelial cells. *Pfluegers Arch.* **428:**569–576
39. Okada, Y. 1997. Volume expansion-sensing outward-rectifier Cl^- channel: fresh start to the molecular identity and volume sensor. *Am. J. Physiol.* **273:**C755–C789
40. O'Neill, W.C. 1999. Physiological significance of volume-regulatory transporters. *Am. J. Physiol.* **276:**C995–C1011
41. Parekh, A.B., Fleig, A., Penner, R. 1997. The store-operated calcium current $I_{(CRAC)}$: nonlinear activation by InsP3 and dissociation from calcium release. *Cell* **89:**973–980
42. Pedersen, S.F., Mills, J.W., Hoffmann, E.K. 1999. Role of the F-actin cytoskeleton in the RVD and RVI processes in Ehrlich ascites tumor cells. *Exp. Cell Res.* **252:**63–74
43. Popp, R., Gogelein, H. 1992. A calcium and ATP sensitive nonselective cation channel in the antiluminal membrane of rat cerebral capillary endothelial cells. *Biochim. Biophys. Acta* **1108:**59–66
44. Poronnik, P., Ward, M.C., Cook, D.I. 1992. Intracellular Ca^{2+} release by flufenamic acid and other blockers of the nonselective cation channel. *FEBS Lett.* **296:**245–248
45. Siemen, D. 1993. Nonselective Cation Channels. *In:* Nonselective Cation Channels. D. Siemen and J.K.-J. Hescheler, editors. pp. 3–25. Birkhäuser Verlag, Basel
46. Siemer, C., Gögelein, H. 1993. Effects of forskolin on crypt cells of rat distal colon. Activation of nonselective cation channels in the crypt base and of a chloride conductance pathway in other parts of the crypt. *Pfluegers Arch.* **424:**321–328
47. Stoos, B.A., Náray-Fejes-Tóth, A., Carretero, O.A., Ito, S., Fejes-Tóth, G. 1991. Characterization of a mouse cortical collecting duct cell line. *Kidney Int.* **39:**1168–1175
48. Strange, K. 1998. Molecular identity of the outwardly rectifying, swelling-activated anion channel: time to reevaluate pICln. *J. Gen. Physiol.* **111:**617–622
49. Strange, K., Emma, F., Jackson, P.S. 1996. Cellular and molecular physiology of volume-sensitive anion channels. *Am. J. Physiol.* **270:**C711–C730
50. Suzuki, M., Miyazaki, K., Ikeda, M., Kawaguchi, Y., Sakai, O. 1993. F-actin network may regulate a Cl^- channel in renal proximal tubule cells. *J. Membrane Biol.* **134:**31–39
51. Szaszi, K., Buday, L., Kapus, A. 1997. Shrinkage-induced protein tyrosine phosphorylation in Chinese hamster ovary cells. *J. Biol. Chem.* **272:**16670–16678
52. Tamaoki, T. 1991. Use and specificity of staurosporine, UCN-01, and calphostin C as protein kinase inhibitors. *Meth. Enzymol.* **201:**340–347
53. Vaca, L., Sinkins, W.G., Hu, Y., Kunze, D.L., Schilling, W.P. 1994. Activation of recombinant trp by thapsigargin in Sf9 insect cells. *Am. J. Physiol.* **267:**C1501–C1505
54. Volk, T., Frömter, E., Korbmacher, C. 1995. Hypertonicity activates nonselective cation channels in mouse cortical collecting duct cells. *Proc. Natl. Acad. Sci. USA* **92:**8478–8482
55. Waldegger, S., Barth, P., Raber, G., Lang, F. 1997. Cloning and characterization of a putative human serine/threonineprotein kinase transcriptionally modified during anisotonic and isotonic alterations of cell volume. *Proc. Natl. Acad. Sci. USA* **94:**4440–4445
56. Wang, W. 1999. Regulation of the ROMK channel: interaction of the ROMK with associate proteins. *Am. J. Physiol.* **277:**F826–F831
57. Wang, W., Giebisch, G. 1991. Dual effect of adenosine triphosphate on the apical small conductance K^+ channel of the rat cortical collecting duct. *J. Gen. Physiol.* **98:**35–61
58. Wehner, F., Sauer, H., Kinne, R.K. 1995. Hypertonic stress increases the Na^+ conductance of rat hepatocytes in primary culture. *J. Gen. Physiol.* **105:**507–535
59. Zhu, X., Chu, P.B., Peyton, M., Birnbaumer, L. 1995. Molecular cloning of a widely expressed human homologue for the Drosophila trp gene. *FEBS Lett.* **373:**193–198